

## Prospects for direct CP tests of $hqq$ interactions

---

Rodrigo Alonso,<sup>a</sup> Cristoforo Fraser-Taliente,<sup>b</sup> Chris Hays,<sup>b</sup> Michael Spannowsky<sup>a</sup>

<sup>a</sup>*Institute for Particle Physics Phenomenology, Department of Physics, Durham University, South Rd, Durham, UK*

<sup>b</sup>*Department of Physics, Oxford University, Keble Rd, Oxford, UK*

ABSTRACT: We study the prospects for probing the CP structure of  $hqq$  interactions using the decays of the lightest baryon  $\Lambda_q$  formed in the quark's hadronization. The low yields of reconstructible events make it unlikely for tests to be performed with the next generation of colliders. In  $h \rightarrow b\bar{b} \rightarrow \Lambda_b\bar{\Lambda}_b$  decays a CP-sensitive distribution could be measured with a high-luminosity  $e^+e^-$  collider, while in both  $h \rightarrow b\bar{b} \rightarrow \Lambda_b\bar{\Lambda}_b$  and  $h \rightarrow c\bar{c} \rightarrow \Lambda_c\bar{\Lambda}_c$  decays such a distribution could be measured with a very high luminosity  $\mu^+\mu^-$  collider. However, we find that only the  $\mu^+\mu^-$  collider can produce enough  $h \rightarrow b\bar{b} \rightarrow \Lambda_b\bar{\Lambda}_b$  decays to probe a physical CP asymmetry in the  $hbb$  vertex.

---

## Contents

<b>1</b>	<b>Introduction</b>	<b>1</b>
<b>2</b>	<b>The decay process</b>	<b>2</b>
2.1	Elementary decay	4
2.2	Hadronization	5
2.3	Hadron decay	6
2.4	Total decay rate	7
2.5	The di-baryon final state	10
<b>3</b>	<b>Experimental sensitivity</b>	<b>12</b>
3.1	$h \rightarrow b\bar{b} \rightarrow \Lambda_b \bar{\Lambda}_b$	13
3.2	$h \rightarrow c\bar{c} \rightarrow \Lambda_c \bar{\Lambda}_c$	14
<b>4</b>	<b>Conclusion</b>	<b>14</b>
<b>A</b>	<b>Massive spinor conventions</b>	<b>15</b>
<b>B</b>	<b>Loss of spin correlation</b>	<b>15</b>
<b>C</b>	<b>Polarization resolution</b>	<b>16</b>

---

## 1 Introduction

The Higgs boson of the Standard Model ( $h$ ) is a CP-even state, and all CP-sensitive measurements are consistent with this hypothesis. These measurements include direct tests of the CP structure of  $hVV$  ( $V = g, W, Z$ ) [1, 2],  $h\tau\tau$  [3], and  $htt$  [4, 5] couplings. Tests of the Higgs boson couplings to other fermions are more challenging, due to the limited measurability of the fermion polarization. They however provide unique sensitivity to sources of new physics, and thus merit investigation. In addition, methods for testing the CP structure of Higgs-boson interactions could be applicable to any new (pseudo)scalar that may be discovered.

The CP structure of the  $hqq$  vertex affects the polarizations of the quark and anti-quark in the  $h \rightarrow q\bar{q}$  decay. For  $b$  and  $c$  quarks we can take  $\Lambda_{QCD}/m_Q \rightarrow 0$  and use heavy-quark effective theory to predict the transfer of the quark spin to the hadron, see e.g. [6]. In the majority of cases this information is lost in the incoherent sum over spin states in hadronization and decay due to parity conservation in QCD and QED. For example, the lowest mass pseudoscalar mesons ( $P_q$ ) have zero spin, so the spin information is lost in the hadronization process. The spin-1 vector mesons ( $P_q^*$ ) preserve polarization information but

it is subsequently lost in the strong decay  $P_q^* \rightarrow P_q\pi$  [7]. Vector-meson decay to polarized photons ( $P_q^* \rightarrow P_q\gamma$ ) preserves spin information, but it is not expected to be observable in foreseen experiments.<sup>1</sup> The measurement of heavy-quark polarization therefore relies on its hadronization to the lightest flavoured baryons ( $\Lambda_q$ ), which decay weakly and preserve the original quark spin in the infinite-mass limit. The  $\Lambda_b$  baryon has previously been used in polarization-sensitive studies of the  $Zbb$  coupling at LEP [9–11], and has been suggested for  $b$ -polarization studies at the LHC [12]. The primary limitations in an analysis of the CP structure of the  $hqq$  vertex are the low rate of baryon production ( $\approx 8\%$  of all heavy-flavour hadrons) and the small fraction of reconstructible baryon decays.

In the following we first summarize the propagation of spin information from the Higgs boson decay to the observable final state, in order to provide a self-contained overview of the process. For this study we employ the massive spinor helicity formalism [13–15], which allows the explicit tracing of spin correlations as well as the reduction of spin  $\geq 1$  representations in terms of spin 1/2 tensor products. For completeness we consider both  $\Lambda_q$  and (vector) meson  $P_q^{(*)}$  production, and show how the formalism provides a simple derivation of the loss of spin information for the latter. We then estimate the rates of production and decay at various future colliders, from which we conclude that CP-sensitive observables may be measured at a  $e^+e^-$  collider with a luminosity upgrade or at a high-energy  $\mu^+\mu^-$  collider, but only the  $\mu^+\mu^-$  collider can produce enough Higgs boson decays to constrain the CP structure of the  $hbb$  vertex.

## 2 The decay process

The progression from the Higgs boson decay to the measured hadron(s) is a three-stage process (Fig. 1), each governed by different forces and scales:

- (i) the *elementary vertex*  $h \rightarrow q\bar{q}$  and the subsequent perturbative QCD radiation;
- (ii) the *hadronization* process, in which the transfer of the (anti-)quark’s polarization to a hadron  $H_q$  ( $\bar{H}_q$ ) is described qualitatively;
- (iii) the *decays of  $H_q$  and  $\bar{H}_q$* , where the distributions of the decay products contain information about the original process.

We assume that any new physics dominantly affects the  $hqq$  vertex, as this is the least explored part of the chain—subsequent processes have been studied experimentally and show no evidence of deviations from the SM. The hard process produces a back-to-back  $q\bar{q}$  pair in the  $h$  rest frame with anti-aligned spins due to angular momentum conservation. In terms of helicity-state amplitudes, the non-vanishing elements are the combinations  $(++)$  or  $(--)$ . As Fig. 2 shows, a CP transformation takes one amplitude into another,  $(--)\leftrightarrow(++)$ , so

---

<sup>1</sup>To measure this polarization one would need to measure the charged tracks from a photon that converts to  $e^+e^-$  in the detector [8]. The fraction of converting photons is expected to be a few percent, and the  $e^+$  and  $e^-$  have very low momentum due to the small mass difference between the vector and scalar mesons.

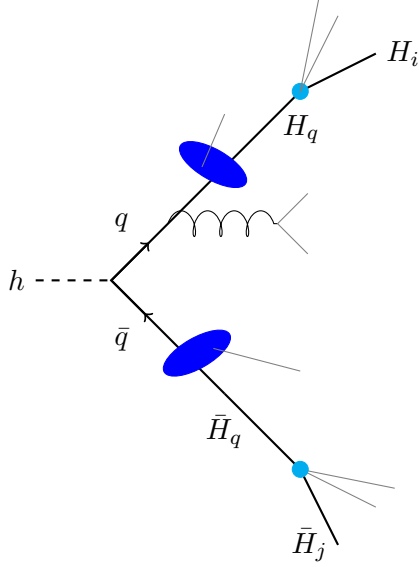


**Figure 1.** The three stages of the decay process: (1) Higgs boson decay ( $h \rightarrow q\bar{q}$ ); (2) hadronization ( $q \rightarrow H_q$ ); and (3) hadron decay ( $H_q \rightarrow H_i X$ ).

to test CP invariance one compares the two amplitudes. They cannot differ arbitrarily, as unitarity requires that they have the same modulus and hence can only differ in their phases. Furthermore these phases change with a rotation around the axis of  $q\bar{q}$  emission, as can be seen by acting with such a transformation on the fermions. This suggests a relationship between CP violation and the relative azimuthal angle (i.e. the angle between the decay planes) of a final-state particle from the decay of  $H_q$  and another from  $\bar{H}_q$ . The particles in the final state selected for our distributions are referred to as polarimeters, and are chosen to balance theoretical sensitivity and experimental reconstructibility.

Throughout the process of  $q\bar{q}$  production, hadronization, and decay, sensitivity to CP violation will be preserved if the state is a coherent superposition of the two helicity amplitudes. In the following we investigate each factorized amplitude,  $\mathcal{A}_{h \rightarrow q\bar{q}}$ ,  $\mathcal{A}_{q \rightarrow H_q}$ , and  $\mathcal{A}_{H_q \rightarrow H_i X}$ , which enter the final amplitude

$$\mathcal{A} = \mathcal{A}_{\bar{H}_q \rightarrow \bar{H}_j \bar{X}} \left[ \mathcal{A}_{\bar{q} \rightarrow \bar{H}_q} (\mathcal{A}_{h \rightarrow q\bar{q}}) \mathcal{A}_{q \rightarrow H_q} \right] \mathcal{A}_{H_q \rightarrow H_i X}, \quad (2.1)$$

with matrix notation and implicit spin indices for the different helicity amplitudes. One of the advantages of the helicity amplitude formalism is that Lorentz invariance allows us to

$$\mathcal{C} \times \left[ \mathcal{P} \times \left( \frac{\bar{q}}{\rightarrow} \bullet \frac{q}{\leftarrow} \right) \right] = \frac{q}{\leftarrow} \bullet \frac{\bar{q}}{\rightarrow} \left[ \right] = \frac{\bar{q}}{\leftarrow} \bullet \frac{q}{\rightarrow} \left| \right.$$

**Figure 2.** Parity and charge transformations on the elementary (--) amplitude. The lines on the arrows represent fermion flow, and the arrows below the lines represent the spin direction.

evaluate each sub-amplitude in the most convenient frame, provided the sum over spin states is performed consistently. Representations of the Lorentz group  $SO(1,3) \sim SU(2)_L \times SU(2)_R$  are given in terms of the irreducible left- and right-handed representations, which are in the irreducible representation of the little group for a massive particle,  $SO(3) \sim SU(2)_{LG}$ . Our notation is

$$\begin{array}{c|ccc} & SU(2)_L & SU(2)_R & SU(2)_{LG} \\ \hline \bar{\alpha} |p^I\rangle & 0 & \mathbf{1/2} & \mathbf{1/2} \\ \alpha |p^I\rangle & \mathbf{1/2} & 0 & \mathbf{1/2} \end{array} \quad |p^I\rangle |p_I| = p_\mu \sigma^\mu \quad \sigma_{\alpha\dot{\alpha}}^\mu = (1, \sigma^i) \quad (2.2)$$

with  $\alpha, \dot{\alpha}$  indices on the Lorentz group,  $I$  a little group index and  $\sigma^i$  the Pauli matrices. The metric for the above indices is the antisymmetric rank-2 tensor  $\epsilon$ . The chiral spinors and conventions are given in Appendix A.

## 2.1 Elementary decay

At the elementary particle level the Higgs boson decay can be derived from the SM  $hq\bar{q}$  vertex and an additional dimension-6 operator,

$$S_{hq\bar{q}} = - \int d^4x \left( y_q \bar{q}_L H q_R + \frac{c_q}{\Lambda^2} H^\dagger H \bar{q}_L H q_R + h.c. \right) \quad (2.3)$$

$$= - \frac{y_q}{\sqrt{2}} \int d^4x \left[ \left( 1 + \frac{3\text{Re}(c_q)v^2}{2y_q\Lambda^2} \right) h\bar{q}q + \frac{3\text{Im}(c_q)v^2}{2y_q\Lambda^2} h\bar{q}\gamma_5 q + \dots \right], \quad (2.4)$$

where  $v = 246$  GeV. The three-point amplitude is

$$(\mathcal{A}_{h \rightarrow \bar{q}q})_{JI} = \frac{m_q}{v} (\zeta [\bar{q}_J q_I] + \zeta^* \langle \bar{q}_J q_I \rangle), \quad \zeta = 1 + \frac{c_q v^2}{y_q \Lambda^2}, \quad (2.5)$$

where the Kronecker delta for colour is omitted, spinors are as given in eq. (2.2), and other conventions are defined in Appendix A.

The above equation can be taken as the starting point as it is the most general three point amplitude and indeed extends beyond the SMEFT case, also comprising HEFT where the expansion around  $\zeta = 1$  need not be a good one. In either case corrections to the quark mass will also be present, such as those implied by eq. (2.3),  $m_q = (y_q v + c_q v^2 / 2\Lambda^2) / \sqrt{2}$ , and accounted for in eq. (2.5).

Taking general expressions for spinors  $|q^I(p)\rangle = \sqrt{\sigma \cdot p} \chi^I$  and  $|q^I(p)] = \sqrt{\bar{\sigma} \cdot p} \chi^I$ , where  $\bar{\sigma}^\mu = (1, -\sigma^i)$  and  $\chi^I$  are the two eigenvectors of spin  $(\vec{S} \cdot \vec{\sigma})$ , one can see that a parity transformation  $P$  swaps angle and square brackets, while charge conjugation  $C$  exchanges  $q \leftrightarrow \bar{q}$ .  $CP$  conservation would then be satisfied for  $\zeta = \zeta^*$ . Unitarity requires the coefficients to be complex conjugates of each other, so the only possible difference is a phase.

The amplitude in matrix notation in the Higgs boson rest frame is

$$\mathcal{A}_{h \rightarrow \bar{q}qI} = \frac{m_q}{v} M_h \begin{pmatrix} \zeta & 0 \\ 0 & -\zeta^* \end{pmatrix}, \quad (2.6)$$

with  $M_h = 125$  GeV.

## 2.2 Hadronization

To model the polarization through the hadronization process, we need a qualitative description of the momentum and spin of the heavy-flavour hadron  $H_q$ . Measurements from LEP indicate that  $H_q$  takes  $\approx 70\%$  of the energy of the quark [16], so we assume that the hadron is produced collinearly with the quark. We take the spin of the heavy quark to be unperturbed by hadronization, as given by the leading-order approximation in HQET. In order to describe the process at the amplitude level we introduce the spin of the light degrees of freedom  $S_\ell$ , which combines with the spin of the heavy quark. The amplitude of the combination of spins that produces a given hadron polarization is determined by Clebsch-Gordan coefficients.

We can derive Clebsch-Gordan coefficients for the projection of  $J_1 \otimes J_2$  onto spin  $J$  states with Lorentz-invariant contractions of  $2J_1$   $J_1$ -spinors,  $2J_2$   $J_2$ -spinors, and  $2J$   $J$ -spinors, albeit all in the rest frame. We can boost to obtain the coefficients in another frame, but then all spinors have the same momentum. This implies a degeneracy in the expression for the Clebsch-Gordan coefficients in terms of spinors. This is partially solved in our case by noting that hadronization must respect parity, so we take

$$\mathcal{A}_{q \rightarrow \Lambda_q} = \frac{a_{\Lambda_q}}{2m_q} (\langle q^I \Lambda_{q,K} \rangle + [\Lambda_{q,K} q^I]) \simeq a_{\Lambda_q} \delta_K^I \quad (2.7)$$

$$\mathcal{A}_{q \rightarrow P_q} = \frac{a_{P_q}}{2m_q} (\langle q^I S_\ell^L \rangle + [S_\ell^L q^I]) \quad (2.8)$$

$$\mathcal{A}_{q \rightarrow P_q^*} = \frac{a_{P_q^*}}{2m_q^2} ([q^I P_{q,K_1}^*] \langle P_{q,K_2}^* S_\ell^L \rangle + [S_\ell^L P_{q,K_1}^*] \langle P_{q,K_2}^* q^I \rangle), \quad (2.9)$$

where the  $K_1, K_2$  indices are symmetrized, and in line with HQET we have approximated the hadron mass to be that of the heavy quark. The use of spinor notation for hadronization will clarify subsequent derivations, such as the loss of spin information for QED and QCD decays. We note that in this notation amplitudes differ not only by an overall scaling and complex phase, but also by a factor of  $\sqrt{2}$  if any  $J_i \geq 1$ . This follows from writing explicitly a sum over an intermediate resonance, e.g. for spin 1:

$$\mathcal{A}_{K_1, K_2} \mathcal{B}^{K_1, K_2} = \mathcal{A}_{K_1, K_2} \mathcal{B}_{K'_1, K'_2} \varepsilon^{K_1, K'_1} \varepsilon^{K_2, K'_2} = \mathcal{A}_{++} \mathcal{B}_{--} + \mathcal{A}_{--} \mathcal{B}_{++} - 2\mathcal{A}_{+-} \mathcal{B}_{+-}. \quad (2.10)$$

Such factors of  $\sqrt{2}$  do not however appear in our final results, since we sum over little group indices.

One can combine the hard process and hadronization to obtain an amplitude with indices for the hadron spin and the light QCD degrees of freedom  $S_\ell$  by summing over the spin indices for the internal quarks  $q$  and using the relations given in Appendix A. The case of a  $\Lambda_q$  baryon is particularly simple with our approximations:

$$\mathcal{A}_{h \rightarrow \Lambda_q \bar{\Lambda}_q X} = \mathcal{A}_{\bar{q} \rightarrow \bar{\Lambda}_q} \mathcal{A}_{h \rightarrow q \bar{q}} \mathcal{A}_{q \rightarrow \Lambda_q} = \frac{m_q M_h a_{\Lambda_q} a_{\bar{\Lambda}_q}}{v} \begin{pmatrix} \zeta & 0 \\ 0 & -\zeta^* \end{pmatrix}. \quad (2.11)$$

### 2.3 Hadron decay

For hadron decay we consider the channels in Fig. 3, which preserve the quark spin information and have sufficiently large branching ratios to be measurable in principle. For a  $\Lambda_q$  baryon we consider either semi-leptonic decays or hadronic decays to a spin-1/2 baryon and one or two pseudoscalar mesons, while for a vector meson  $P_q^*$  we consider the electromagnetic decay.

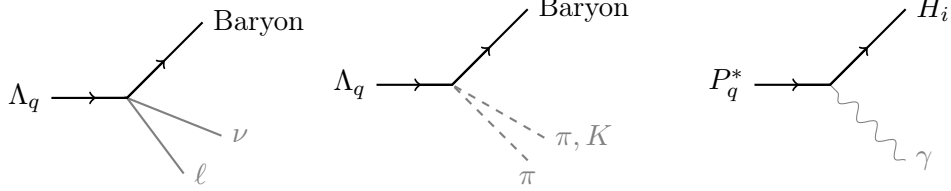


**Figure 3.** The considered weak baryon decays (left two diagrams) and electromagnetic vector meson decay (right diagram).

For semi-leptonic decays the HQET limit implies that the chiral structure of weak interactions will be passed on to the amplitude for the  $\Lambda_q$  baryon, so the amplitude is

$$\mathcal{A}_{\Lambda_b \rightarrow \Lambda_i \ell \bar{\nu}} = \frac{4G_F V_{ib}}{\sqrt{2}} f_{1b}(q^2) [\Lambda_i | \bar{\sigma}_\mu | \Lambda_b] J_{\ell \bar{\nu}}^\mu = \frac{8G_F V_{ib}}{\sqrt{2}} f_{1b}(q^2) [\Lambda_i \ell] \langle \bar{\nu} | \Lambda_b \rangle, \quad (2.12)$$

$$\mathcal{A}_{\Lambda_c \rightarrow \Lambda_i \ell \bar{\nu}} = \frac{4G_F V_{ci}^*}{\sqrt{2}} f_{1c}(q^2) [\Lambda_i | \bar{\sigma}_\mu | \Lambda_c] J_{\ell \bar{\nu}}^\mu = \frac{8G_F V_{ci}^*}{\sqrt{2}} f_{1c}(q^2) [\Lambda_i \nu] \langle \bar{\ell} | \Lambda_c \rangle, \quad (2.13)$$

with  $J_{\ell \bar{\nu}}^\mu = [\ell | \bar{\sigma}^\mu | \bar{\nu}]$ ,  $J_{\ell \bar{\nu}}^\mu = [\nu | \bar{\sigma}^\mu | \bar{\ell}]$ . The decay amplitude for anti-baryons is obtained from the hermitian conjugate, which exchanges angle and square brackets (see Appendix A).

For a fully hadronic decay to a baryon  $\Lambda_i$  and a pion, the factorized amplitude is

$$\mathcal{A}_{\Lambda_q \rightarrow \Lambda_i \pi} = \frac{4G_F V_{iq}}{\sqrt{2}} f_{1q} [\Lambda_i | \bar{\sigma}_\mu | \Lambda_q] f_\pi q^\mu \simeq \frac{4G_F}{\sqrt{2}} G_F f_{1q} f_\pi m_{\Lambda_q} [\Lambda_i \Lambda_q] \quad (2.14)$$

where the  $\Lambda_i$  baryon mass is neglected in the second equality. At this order kinematics implies that the spins of both  $\pi$  and  $\Lambda_i$  are correlated with the  $\Lambda_q$  spin. For the charm quark the  $\Lambda_c \rightarrow p K \pi$  decay is experimentally accessible. Here the applicability of the factorization hypothesis is not as well motivated. However, Bjorken has argued [17], and experimental data [18] suggest, that the spin directions of the kaon and  $\Lambda_c$  are anti-correlated (as is the case for  $\Lambda$  in  $\Lambda_c \rightarrow \Lambda \bar{\ell} \nu$  decays). Thus, the  $\Lambda_c \rightarrow p K \pi$  decay is expected to be a viable mode for studies of spin correlations.

In all of the above expressions the particle whose spin is directly correlated with that of the decaying hadron is the one with the same angle  $\langle \rangle$  or square bracket  $[\ ]$  product. This indicates the ideal polarimeter in theory, although in practice its detection might not be possible.

It is useful to collect all the above decay amplitudes into the expression

$$\mathcal{A}_{\Lambda_q \rightarrow \Lambda_i X} = \frac{4G_F V_{iq}}{\sqrt{2}} [\Lambda_i | \bar{\sigma}_\mu | \Lambda_q] J_X^\mu \left\{ \begin{array}{l} J_\pi^\mu = f_{1q}(0) f_\pi q^\mu \\ J_{\ell \bar{\nu}}^\mu = f_{1q}(q^2) [\ell | \bar{\sigma}^\mu | \bar{\nu}] \\ J_{\ell \bar{\nu}}^\mu = f_{1q}(q^2) [\nu | \bar{\sigma}^\mu | \bar{\ell}] \end{array} \right\}, \quad (2.15)$$

with the substitution  $V_{iq} \rightarrow V_{qi}^*$  if the heavy quark is charm, and where we have neglected the pion mass.

Lastly for the electromagnetic decay of a vector meson one has:

$$\mathcal{A}_{P_q^* \rightarrow \gamma^- P_q} = ef_\gamma \frac{\langle P_q^* \gamma \rangle^2}{m_{P_q^*}}, \quad \mathcal{A}_{P_q^* \rightarrow \gamma^+ P_q} = ef_\gamma \frac{[P_q^* \gamma]^2}{m_{P_q^*}}. \quad (2.16)$$

with the superscript  $\pm$  representing polarization and with the same coefficient for both amplitudes, as required by parity. Combining the fragmentation and decay amplitudes gives

$$\mathcal{A}_{q \rightarrow P_q^*} \mathcal{A}_{P_q^* \rightarrow P_q \gamma^+} = -ef_\gamma a_{P_q^*} m_q [S_\ell^L \gamma] [q^I \gamma] \quad (2.17)$$

$$\mathcal{A}_{q \rightarrow P_q^*} \mathcal{A}_{P_q^* \rightarrow P_q \gamma^-} = ef_\gamma a_{P_q^*} m_q \langle S_\ell^L \gamma \rangle \langle q^I \gamma \rangle \quad (2.18)$$

where we have equated the heavy quark and hadron masses, and summed over quark spin states. There still remains however the sum over the light QCD degrees of freedom  $S_\ell$  in the squared amplitude; this sum together with the sum over photon polarizations washes away spin information, as shown in Appendix B. Thus, one must measure the photon polarization to access the spin information of the decaying particle.

## 2.4 Total decay rate

We finally give the rate for the full process, making explicit the little group (spin) indices that are usually left implicit in favour of the Lorentz group  $SU(2)_L \times SU(2)_R$  structure. The two forms are equivalent and here we choose the former in order to write sub-amplitudes in the frame where they are simplest. One has then

$$d\Gamma = \frac{3d\Phi_{H_q} d\Phi_{\bar{H}_q}}{16\pi M_h (2m_{H_q})^2 \Gamma_{H_q}^2} \sum \left[ \left( \mathcal{A}_{H_q \rightarrow H_i X} \mathcal{A}_{H_q \rightarrow H_i X}^\dagger \right)_{\{I\}}^{\{K\}} \left( \mathcal{A}_{\bar{H}_q \rightarrow \bar{H}_j X}^\dagger \mathcal{A}_{\bar{H}_q \rightarrow \bar{H}_j X} \right)_{\{J\}}^{\{L\}} \right. \\ \left. \times \left( \mathcal{A}_{h \rightarrow \bar{q} q \rightarrow \bar{H}_q H_q}^\dagger \right)^{\{I\}, \{J\}} \left( \mathcal{A}_{h \rightarrow \bar{q} q \rightarrow \bar{H}_q H_q} \right)_{\{L\}, \{K\}} \right] \quad (2.19)$$

$$= \frac{3d\Phi_{H_q} d\Phi_{\bar{H}_q}}{16\pi M_h (2m_{H_q})^2 \Gamma_{H_q}^2} \sum \left[ \left( \mathcal{A}_{q \rightarrow H_i X} \mathcal{A}_{q \rightarrow H_i X}^\dagger \right)_I^K \left( \mathcal{A}_{\bar{q} \rightarrow \bar{H}_j X}^\dagger \mathcal{A}_{\bar{q} \rightarrow \bar{H}_j X} \right)_J^L \right. \\ \left. \times \left( \mathcal{A}_{h \rightarrow \bar{q} q}^\dagger \right)^{IJ} \left( \mathcal{A}_{h \rightarrow \bar{q} q} \right)_{LK} \right], \quad (2.20)$$

where  $d\Phi$  stands for Lorentz invariant phase space and raised indices follow from the complex conjugation relations given in Appendix A. The indices in the first expression represent spin states of the hadron, and in the second expression they represent spin states of the quark-antiquark pair produced in the original process. The latter provides the information contained in the original vertex: eq. (2.6) shows that in the Higgs rest frame the amplitude is diagonal in helicity indices and CP-violation is encoded in the relative phase of the two entries. For a CP-violating effect one therefore needs interference, i.e. off-diagonal elements  $K \neq I$ ,  $J \neq L$  in



the product of hadronization and decay amplitudes. For QCD and QED decays these elements vanish and no spin information can be extracted, as shown in ref. [7]; we derive this result in Appendix B using the parity of QCD and QED interactions and the spinor notation.

Interference is also lost when integrating over all phase space, since the rate collapses to a single sum over the square of amplitudes, that is

$$\Gamma = \sum_{I,J} \int \frac{3d\Phi_{H_q} d\Phi_{\bar{H}_q}}{16\pi M_h (2m_{H_q})^2 \Gamma_{H_q}^2} \left[ \left( \mathcal{A}_{H_q \rightarrow H_i X} \mathcal{A}_{H_q \rightarrow H_i X}^\dagger \right)_{\{I\}}^{\{I\}} \left( \mathcal{A}_{\bar{H}_q \rightarrow \bar{H}_j X} \mathcal{A}_{\bar{H}_q \rightarrow \bar{H}_j X}^\dagger \right)_{\{J\}}^{\{J\}} \right. \\ \left. \times \left( \mathcal{A}_{h \rightarrow \bar{q} q \rightarrow \bar{H}_q H_q}^\dagger \right)_{\{I\}\{J\}}^{\{I\}\{J\}} \left( \mathcal{A}_{h \rightarrow \bar{q} q \rightarrow \bar{H}_q H_q} \right)_{\{J\}\{I\}} \right] \quad (2.21)$$

$$= \sum_{IJ} \Gamma_{h \rightarrow \bar{q} q \rightarrow H_q^{\{I\}} \bar{H}_q^{\{J\}}} \text{Br}(H_q^{\{I\}} \rightarrow H_i X) \text{Br}(\bar{H}_q^{\{J\}} \rightarrow \bar{H}_j X), \quad (2.22)$$

at which point there is no direct CP sensitivity. We thus need a differential decay rate, which we define as a function of three angles: the polar angles of the two particles that we select as polarimeters,  $\theta$  and  $\bar{\theta}$ , and their relative azimuthal angle  $\delta\phi = \phi - \bar{\phi}$ . The former is defined in the rest frame of the decaying  $H_q$  hadron, while the latter is invariant under a boost in the quark-antiquark direction. These angles and their change under a CP transformation are shown in Fig. 4.

To summarize,  $\Lambda_q$  production is the single channel preserving quark spin information, and the differential angular decay rate  $d\Gamma/d\Omega d\bar{\Omega}$  is required to directly test for CP violation. It is useful to decompose the helicity structure of the hadron decay rate as

$$d\Gamma_{H_q(\hat{s})} \equiv (d\Gamma_{H_q} + d\Gamma_L \hat{s}_L + (d\Gamma_+ \hat{s}_- + c.c.)), \quad (2.23)$$

where  $\hat{s} = \langle\langle \vec{\mathbf{S}} \rangle\rangle / |\langle\langle \vec{\mathbf{S}} \rangle\rangle|$  is the hadron spin direction,  $\hat{s}_- = \hat{s}_\perp - i\hat{s}_T$ ,  $\mathbf{S}$  is the spin operator, and

$$d\Gamma_{H_q} = \frac{d\Phi}{2m_{H_q}} \frac{1}{2} \left[ \left( \mathcal{A}_{H_q \rightarrow H_i X} \mathcal{A}_{H_q \rightarrow H_i X}^\dagger \right)_+^+ + \left( \mathcal{A}_{H_q \rightarrow H_i X} \mathcal{A}_{H_q \rightarrow H_i X}^\dagger \right)_-^- \right] = \frac{1}{2} \text{Tr} (d\Gamma_{H_q}(\hat{s})) \\ d\Gamma_L = \frac{d\Phi}{2m_{H_q}} \frac{1}{2} \left[ \left( \mathcal{A}_{H_q \rightarrow H_i X} \mathcal{A}_{H_q \rightarrow H_i X}^\dagger \right)_+^+ - \left( \mathcal{A}_{H_q \rightarrow H_i X} \mathcal{A}_{H_q \rightarrow H_i X}^\dagger \right)_-^- \right] = \frac{1}{2} \text{Tr} (\mathbf{S}_L d\Gamma_{H_q}(\hat{s})) \\ d\Gamma_+ = \frac{d\Phi}{2m_{H_q}} \frac{1}{2} \left( \mathcal{A}_{H_q \rightarrow H_i X} \mathcal{A}_{H_q \rightarrow H_i X}^\dagger \right)_-^+ = \frac{1}{4} \text{Tr} ((\mathbf{S}_\perp + i\mathbf{S}_T) d\Gamma_{H_q}(\hat{s})). \quad (2.24)$$

The perpendicular and transverse components  $d\Gamma_{\perp,T}$  are twice the real or imaginary part of  $d\Gamma_+$ ,

$$d\Gamma_\perp = d\Gamma_+ + c.c. \quad d\Gamma_T = -id\Gamma_+ + c.c. \quad (2.25)$$

and we group the three terms into  $d\Gamma_i = d\Gamma_\perp, d\Gamma_T, d\Gamma_L$ . For concreteness we can assign  $(\perp, T, L)$  to a frame  $(x, y, z)$  while bearing in mind that the polarization for the anti-hadron will have assignments to that frame with relative signs determined by the translation from helicity to spin.

With these definitions and the form of the elementary vertex in eq. (2.6) the rate is:

$$d\Gamma = \frac{3M_h d\Gamma_{H_q} d\Gamma_{\bar{H}_q} m_q^2 |\zeta|^2}{8\pi \Gamma_{H_q} \Gamma_{\bar{H}_q} v^2} \left( 1 + \frac{d\Gamma_L d\bar{\Gamma}_L}{d\Gamma_{H_q} d\bar{\Gamma}_{\bar{H}_q}} - 2 \frac{\zeta}{\zeta^*} \frac{d\Gamma_+ d\bar{\Gamma}_+}{d\Gamma_{H_q} d\bar{\Gamma}_{\bar{H}_q}} + c.c. \right). \quad (2.26)$$

It is useful to rewrite this expression in terms of spin correlations and contrast with Higgs boson decay to  $Z$  bosons. One has for Higgs bosons no net polarization for a given fermion, i.e. tracing over the spin states of other Higgs decay products leaves the remaining particle unpolarized, contrary to  $Z$  boson decay. To retain polarization information one must therefore keep track of the spin of both decay products. Explicitly, the density matrix of elementary particles after Higgs boson decay is:

$$(\rho_q)_I^{I'} \otimes (\rho_{\bar{q}})_{J'}^{J'} = \frac{\int (\mathcal{A}_{h \rightarrow q\bar{q}})_{JI} (\mathcal{A}_{h \rightarrow q\bar{q}}^\dagger)^{I'J'} d\Phi}{\int (\mathcal{A}_{h \rightarrow q\bar{q}})_{KL} (\mathcal{A}_{h \rightarrow q\bar{q}}^\dagger)^{KL} d\Phi} \quad (2.27)$$

which one can decompose in terms of spin operators as

$$\rho_q \otimes \rho_{\bar{q}} = \frac{\mathbb{I}}{2} \otimes \frac{\mathbb{I}}{2} + \frac{\mathbb{I}}{2} \otimes \vec{\mathcal{P}}_{\bar{q}} \cdot \vec{\mathbf{S}} + \vec{\mathcal{P}}_q \cdot \vec{\mathbf{S}} \otimes \frac{\mathbb{I}}{2} + \mathcal{T}_{ij} \mathbf{S}^i \otimes \mathbf{S}^j. \quad (2.28)$$

It is then straightforward to check that  $\vec{\mathcal{P}}_q = \vec{\mathcal{P}}_{\bar{q}} = 0$ , so that tracing over one of the fermions leaves the other unpolarized. The correlation between spins is

$$\mathcal{T} = - \begin{pmatrix} \cos(\text{Arg}(2\zeta)) & -\sin(\text{Arg}(2\zeta)) & 0 \\ \sin(\text{Arg}(2\zeta)) & \cos(\text{Arg}(2\zeta)) & 0 \\ 0 & 0 & 1 \end{pmatrix} \quad (2.29)$$

with spin as measured in the  $q$  and  $\bar{q}$  rest frames but with the axes of both frames aligned (this means that the explicit operator form of  $\mathbf{S}$  acting on  $q$  and  $\bar{q}$  helicity states is different).

In terms of the spin correlation the rate is

$$d\Gamma = \frac{3M_h d\Gamma_{H_q} d\Gamma_{\bar{H}_q} m_q^2 |\zeta|^2}{8\pi \Gamma_{H_q} \Gamma_{\bar{H}_q} v^2} \left( 1 + \frac{d\Gamma^i}{d\Gamma_{\Lambda_q}} \mathcal{T}_{ij} \frac{d\bar{\Gamma}^j}{d\bar{\Gamma}_{\bar{\Lambda}_q}} \right). \quad (2.30)$$

If the polarization fraction retained by the hadron  $r_i$  [12] is less than one, this can be implemented by the replacement  $\mathcal{T}_{ij} \rightarrow r_i \mathcal{T}_{ij} r_j$ .

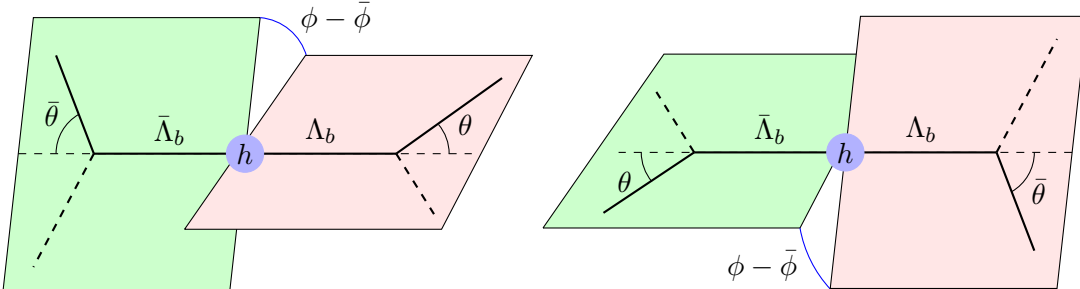


**Figure 4.** CP transformation under which  $\theta \leftrightarrow \bar{\theta}$  and  $\phi \rightarrow \bar{\phi} + \pi, \bar{\phi} \rightarrow \phi + \pi$ . The polar angle is defined with respect to the axis given by the  $\Lambda_b$  momentum.

## 2.5 The di-baryon final state

We focus on the experimentally viable  $\Lambda_q \times \bar{\Lambda}_q$  final state and neglect the effect of excited baryon states that slightly dilute the polarization information [12]. The procedure is to select a final-state particle to serve as the polarimeter and integrate over the phase space of the remaining particles. The contribution of each secondary decay to the rate is

$$d\Phi_H \left( \mathcal{A}_{H_q \rightarrow H_i X} \mathcal{A}_{H_q \rightarrow H_i X}^\dagger \right)_J^I \equiv \langle \Lambda_q^I | \sigma_\mu | \Lambda_{q,J} \rangle dK^\mu \quad (2.31)$$

$$d\Phi_{\bar{H}} \left( \mathcal{A}_{\bar{H}_q \rightarrow \bar{H}_j X}^\dagger \mathcal{A}_{\bar{H}_q \rightarrow \bar{H}_j X} \right)_L^K \equiv -\langle \bar{\Lambda}_{q,L} | \sigma_\mu | \bar{\Lambda}_q^K \rangle d\bar{K}^\mu \quad (2.32)$$

where the sign is due to the complex conjugation of spinors and little group indices, see Appendix A. The four-vector  $dK^\mu$  is proportional to a combination of the polarimeter momentum and that of the  $\Lambda_q$  baryon. The highest sensitivity is achieved when the  $p_{\Lambda_q}$  component is zero; for semileptonic decays the amplitudes in eqs. (2.12) and (2.13) show that this would imply maximal sensitivity for neutrinos from  $\Lambda_b$  decay and charged leptons from  $\Lambda_c$  decay.

The currents  $dK^\mu$  for various decays and choices of polarimeter particle are

$$\Lambda_b \rightarrow \Lambda_c \pi : \quad dK_\pi^\mu = \frac{(2\pi)^2 f_{1b}^2(0) f_\pi^2}{m_{\Lambda_b}} \frac{1 - \delta}{1 + \delta} p_\pi^\mu \frac{C_{cb} d^3 p_\pi}{2E_\pi (2\pi)^3} \delta(m_{\Lambda_b} - E_{\Lambda_c} - E_\pi) \quad (2.33)$$

$$\Lambda_b \rightarrow \Lambda_c \bar{\nu} \ell : \quad dK_{\bar{\nu}}^\mu = \hat{f}_{1b}^2(x) \frac{(y-x)}{y^2} \left[ x p^\mu + \left( 1 - \delta + x - y - \frac{2x}{y} \right) p_\ell^\mu \right] \frac{C_{cb} dx d^3 p_\ell}{2E_\ell (2\pi)^3} \quad (2.34)$$

$$\Lambda_c \rightarrow \Lambda \nu \bar{\ell} : \quad dK_{\bar{\nu}}^\mu = \hat{f}_{1c}^2(x) \frac{(1-\delta-y)}{y} p_\ell^\mu \frac{C_{cs} dx d^3 p_\ell}{2E_\ell (2\pi)^3} \quad (2.35)$$

$$\Lambda_c \rightarrow \Lambda \nu \bar{\ell} : \quad dK_\Lambda^\mu = \frac{\hat{f}_{1c}^2(x)}{6} \left[ (1-\delta-x)(p-p_\Lambda)^\mu + x p_\Lambda^\mu \right] \frac{C_{cs} dp_\Lambda^3}{2E_k (2\pi)^3} \quad (2.36)$$

where

$$x = \frac{q^2}{m_{\Lambda_q}^2}, \quad y = \frac{2p_\ell \cdot p}{m_{\Lambda_q}^2}, \quad \delta = \frac{m_{\Lambda_i}^2}{m_{\Lambda_j}^2}, \quad \hat{f}(x) = f(m_{\Lambda_q}^2 x), \quad C_{ij} = \frac{4|V_{ij}|^2 G_F^2 m_{\Lambda_q}^2}{\pi}. \quad (2.37)$$

The inclusive semi-leptonic case can be obtained from the above in the leading approximation with the substitutions  $f \rightarrow 1$  and  $\delta = m_c^2/m_b^2, m_s^2/m_c^2$ .

Given the expressions for the  $\Lambda_b$  spinor in its rest frame and the decomposition in eq. (2.24), the average over + and - helicities selects the time-like component of  $dK^\mu$ . The longitudinal contribution  $d\Gamma_L$  selects the component along the  $\bar{\Lambda}_b$  direction ( $dK_L \propto \cos \theta$ ), whereas  $d\Gamma_+$  selects normal components ( $K_\perp + iK_T \propto \sin \theta e^{i\phi}$ ). The ideal polarimeter has the most sensitive angular distribution, which translates into the largest time-like to space-like component ratio in  $dK^\mu$ . This is conventionally encoded in the spin resolution power,  $\alpha$ , which here is defined as

$$\frac{d\Gamma}{d \cos \theta_n} = \frac{\Gamma}{2} (1 + \alpha_n \cos \theta_n) \quad \alpha_n = \frac{3 \int \cos \theta_n d\Gamma}{\int d\Gamma}, \quad (2.38)$$

with  $\theta_n$  the angle between the polarimeter particle  $n$  and the hadron spin direction, and the factor of 3 is for normalization. The parameter  $\bar{\alpha}$  is defined similarly for the  $\bar{\Lambda}_b$  case. Dividing the Higgs boson decay rate by  $\Gamma_{q\bar{q}}$  gives the angular differential decay rate,

$$\begin{aligned}
\frac{(4\pi)^2}{\Gamma_{h\rightarrow q\bar{q}}} \frac{d\Gamma_{h\rightarrow\Lambda_i X \bar{\Lambda}_j X'}}{d\Omega d\bar{\Omega}} &= \text{Br}_{\Lambda_q\rightarrow\Lambda_i X} \text{Br}_{\bar{\Lambda}_q\rightarrow\bar{\Lambda}_j X'} f_{\Lambda_q}^2 \left( 1 + \frac{d\Gamma^i}{d\Gamma_{\Lambda_q}} \mathcal{T}_{ij} \frac{d\bar{\Gamma}^j}{d\bar{\Gamma}_{\bar{\Lambda}_q}} \right) \\
&= \text{Br}_{\Lambda_q\rightarrow\Lambda_i X} \text{Br}_{\bar{\Lambda}_q\rightarrow\bar{\Lambda}_j X'} f_{\Lambda_q}^2 \left( 1 + \frac{d\Gamma_L d\bar{\Gamma}_L}{d\Gamma_{\Lambda_q} d\bar{\Gamma}_{\bar{\Lambda}_q}} - 2 \frac{\zeta^*}{\zeta} \frac{d\Gamma_+ d\bar{\Gamma}_+}{d\Gamma_{\Lambda_q} d\bar{\Gamma}_{\bar{\Lambda}_q}} + c.c. \right), \\
&= \text{Br}_{\Lambda_q\rightarrow\Lambda_i X} \text{Br}_{\bar{\Lambda}_q\rightarrow\bar{\Lambda}_j X'} f_{\Lambda_q}^2 \left[ 1 + \alpha_n \bar{\alpha}_m \left( c_\theta c_{\bar{\theta}} + \text{Re} \left( \frac{\zeta^*}{\zeta} e^{i\delta\phi} \right) s_\theta s_{\bar{\theta}} \right) \right],
\end{aligned} \tag{2.39}$$

where the angular coordinates  $\Omega$  and  $\bar{\Omega}$  are defined in the rest frames of  $\Lambda_q$  and  $\bar{\Lambda}_q$ , respectively,  $\delta\phi = \phi - \bar{\phi}$  has the orientation shown in Fig. 4, and  $f_{\Lambda_q}$  is the fragmentation ratio into  $\Lambda_q$ , which is  $\approx 7\%$  for  $b$  quarks [19] and  $\approx 8\%$  for  $c$  quarks [20].

The ratios  $\alpha_a$  determine the quality of our polarimeter particle and are as follows (the particle used as the polarimeter is highlighted in blue):

	$\Lambda_b \rightarrow \Lambda_c \ell \nu$	$\Lambda_b \rightarrow X_c \ell \nu$	$\Lambda_c \rightarrow \Lambda \ell \nu$ or $\pi \Lambda$	$\Lambda_c \rightarrow X_s \ell \nu$	$\Lambda_c \rightarrow p K \pi$ or $\Lambda \ell \nu$
$\alpha$	-0.4	-0.3	1, 1	1	-0.2, -0.4
$\bar{\alpha}$	0.4	0.3	-1, -1	-1	0.2, 0.4

Due to the chiral structure of the weak interaction, the optimal polarimeters have opposite isospin to the decaying quark, as evident in the right-hand side of eqs. (2.12) and (2.13). Polarimeters with the same isospin retain correlations through momentum conservation, and for these  $\alpha_a$  can be calculated from phase space integrals (see Appendix C). Except for  $pK\pi$ , which is taken from [18], the above values are rough estimates determined using our approximations and formalism, though both experimental and more precise theory inputs are available [19]. The relative sign  $\bar{\alpha} = -\alpha$  can be understood intuitively from the weak group chirality: if a given decay involves a (massless) polarimeter particle with one helicity, the weak interactions in the conjugate process select the opposite helicity for the anti-particle (hence a flipped sign).

To define a CP-odd observable we subtract the CP conjugate,

$$\mathcal{CP}(d\Gamma)(\mathcal{CP})^{-1} = d\Gamma^{CP} = d\Gamma(n \rightarrow \bar{m}, m \rightarrow \bar{n}, \theta \leftrightarrow \bar{\theta}, \phi \leftrightarrow \bar{\phi}), \tag{2.40}$$

where a bar indicates the antiparticles of the original decay product.

Normalizing to the total rate, the relative differential rate of CP violation is

$$\frac{d\Gamma - d\Gamma^{CP}}{\Gamma + \Gamma^{CP}} = \alpha_n \bar{\alpha}_m \sin(2\text{Arg}\zeta) \sin(\phi - \bar{\phi}) \sin\theta \sin\bar{\theta} \frac{d\Omega_n d\bar{\Omega}_m}{(4\pi)^2}. \tag{2.41}$$

To experimentally probe CP, we integrate over the CP-sensitive observable to obtain the number of events with a given sign,

$$N_{\pm} \equiv N[\vec{p}_m \cdot (\vec{p}_n \wedge \vec{p}_{\Lambda_b}) \gtrless 0], \quad N_{\pm}^{CP} \equiv N^{CP}[\vec{p}_{\bar{n}} \cdot (\vec{p}_{\bar{m}} \wedge \vec{p}_{\Lambda_b}) \gtrless 0], \tag{2.42}$$

as measured in the Higgs boson rest frame. The integrated asymmetry is then

$$\epsilon_{CP}^{nm} = \frac{N_+ - N_- + N_+^{CP} - N_-^{CP}}{N_+ + N_- + N_+^{CP} + N_-^{CP}}, \quad (2.43)$$

which corresponds to

$$\epsilon_{CP}^{nm} \equiv \left[ \int_{\sin(\phi-\bar{\phi})>0} - \int_{\sin(\phi-\bar{\phi})<0} \right] \frac{d\Gamma - d\Gamma^{CP}}{2\Gamma} = \frac{\pi\alpha_n\bar{\alpha}_m \sin(2\text{Arg}\zeta)}{8}. \quad (2.44)$$

Given the small fragmentation into  $\Lambda_q$ , considering multiple decay channels can increase yields, although general considerations require  $-1 \leq \alpha \leq 1$  for each channel.

Finally, for an alternative derivation of the CP-violating effect, rather than writing amplitudes for every subprocess we can carry out the spin sums connecting the different vertices. Using eq. (2.15) and the completeness relation

$$|\Lambda_{q,K}\rangle (\zeta^* \langle \Lambda_q^K \bar{\Lambda}_q^L | + \zeta [\Lambda_q^K \bar{\Lambda}_q^L]) |\bar{\Lambda}_{q,L}\rangle = (\zeta^* m_{\Lambda_q} p_{\Lambda_q}^\mu \sigma_\mu - \zeta m_{\Lambda_q} p_{\Lambda_q}^\mu \sigma_\mu) \equiv m_{\Lambda_q} \hat{\zeta}_\mu \sigma^\mu, \quad (2.45)$$

the general differential decay rate reads

$$d\Gamma = \mathcal{N} \text{Tr} (\bar{\sigma}_\mu \sigma_\alpha \bar{\sigma}_\nu \sigma_\beta) dK_n^\mu d\bar{K}_m^\nu \hat{\zeta}^\alpha \hat{\zeta}^{*\beta} \left\{ \begin{array}{l} K_\pi^\mu = f_\pi (p_\pi \cdot p_{\Lambda_i}) p_\pi^\mu \\ K_{\nu\ell}^\mu = f(q^2) [(m_{\Lambda_q}^2 - q^2) q^\mu + q^2 p_{\Lambda_i}^\mu] \end{array} \right\} \quad (2.46)$$

with the Lorentz structure that gives rise to CP violation appearing in the Levi-Civita tensor that results from tracing over  $\sigma^\mu$  matrices.

### 3 Experimental sensitivity

Given the ability to model the progression of CP information from the Higgs-boson decay to the final-state particles, we next investigate the potential experimental sensitivity to the CP structure of  $hqq$  interactions at future colliders. We focus on  $hbb$  and  $hcc$  interactions, for which heavy-quark effective theory can be used. Approximately one in  $10^6$   $h \rightarrow q\bar{q}$  decays are reconstructible for a CP test because of the fragmentation of both quarks into baryons ( $\approx 1\%$ ), the branching ratios for both baryons to decay into measurable final states ( $\approx 1\%$ ), and the reconstruction acceptance ( $\approx 1\%$ ). The analysis thus requires  $> 10^8$  Higgs-boson events, which could be produced by a high-luminosity  $pp$ ,  $e^+e^-$ , or  $\mu^+\mu^-$  collider.

The proposed FCC-hh would provide an integrated luminosity of  $20 \text{ ab}^{-1}$  of  $\sqrt{s} = 100 \text{ TeV}$   $pp$  collisions in each of two detectors over a span of two and a half decades [21]. To study the  $h \rightarrow q\bar{q}$  decay, the  $h\ell\nu$  and  $h\ell\ell$  ( $\ell = e, \mu$ ) production processes would be needed to avoid the large QCD multijet backgrounds. Combining the respective cross sections of  $3.4 \text{ pb}$  and  $0.75 \text{ pb}$  [22, 23], and the yields of two experiments, gives a total of 170 million Higgs boson events.

The FCC-ee collider would provide an integrated luminosity of  $5 \text{ ab}^{-1}$  of  $\sqrt{s} = 240 \text{ GeV}$   $e^+e^-$  collisions at two collision points in three years of operation [24]. This would be insufficient to probe CP-violation in the  $hqq$  interaction, so we consider a high-luminosity  $e^+e^-$

collider [25] that would produce five times the instantaneous luminosity of the FCC-ee and would run for the same duration as the FCC-hh. With the resulting  $200 \text{ ab}^{-1}$  of integrated luminosity in each of four detectors, and the  $e^+e^- \rightarrow Zh$  cross section of  $200 \text{ fb}$  [24], a similar number of Higgs bosons would be produced as for the FCC-hh  $h\nu$  and  $h\ell\ell$  processes.

A muon collider [26] offers the potential for high-energy collisions at high luminosity. Two speculative scenarios under investigation [27] that would produce sufficient Higgs boson yields are  $\sqrt{s} = 30 \text{ TeV}$  and  $100 \text{ TeV}$   $\mu^+\mu^-$  colliders with  $90 \text{ ab}^{-1}$  and  $1000 \text{ ab}^{-1}$  of integrated luminosity, respectively, for five years of running. The cross section for Higgs boson production through vector-boson fusion is  $1.2 \text{ pb}$  for  $\sqrt{s} = 30 \text{ TeV}$  [28], and extrapolating the logarithmic growth with energy to  $100 \text{ TeV}$  gives a cross section of  $1.4 \text{ pb}$ . The expected Higgs-boson yields are thus 110 million to 1.4 billion per detector.

### 3.1 $h \rightarrow b\bar{b} \rightarrow \Lambda_b \bar{\Lambda}_b$

The multistage decay of  $\Lambda_b \rightarrow \Lambda_c X \rightarrow \Lambda X'$  precludes the full reconstruction of the  $\Lambda_b$  baryon with high efficiency. In order to maximize the event yield, we consider a partial  $\Lambda_b$  reconstruction that requires only a charged lepton (to provide polarization information) and a  $\Lambda$  baryon (to provide discrimination from other hadrons). This final state was successfully used in measurements of  $Z \rightarrow b\bar{b}$  decays at LEP [29–31].

We estimate the expected event yields for  $h \rightarrow \Lambda_b \bar{\Lambda}_b \rightarrow \Lambda \ell \nu \bar{\Lambda} \ell \nu X$  using the 57.5%  $h \rightarrow b\bar{b}$  branching fraction and the  $0.65 \pm 0.08\%$  rate measured by ALEPH for  $b \rightarrow \Lambda_b \rightarrow \Lambda \ell \nu X$  ( $\ell = e, \mu$ ) [29]. Combining these factors gives a total of  $24 \pm 3$  events per million Higgs bosons produced. The yield is further reduced by the 64% branching fraction of the observable  $\Lambda \rightarrow p\pi$  decay, giving  $10 \pm 1$  events with a measurable  $\Lambda \ell^+ \bar{\Lambda} \ell^-$  final state per million Higgs bosons.

Given the small event yields, sensitivity is only possible if the backgrounds are very low. This makes the FCC-hh insensitive, since  $h \rightarrow b\bar{b}$  measurements are background-dominated in  $pp$  collisions [32, 33]. The analysis may however be feasible in the low-background environment of an  $e^+e^-$  [34] or a  $\mu^+\mu^-$  [28] collider.

We estimate the acceptance for selecting events in  $e^+e^-$  collisions using a sample of  $e^+e^- \rightarrow ZH$  events generated with Madgraph\_aMC@NLO [35] + Pythia 6.428 [36] at leading order. We do not include detector resolutions and efficiencies, which will need to be high to have CP sensitivity—the primary challenge will be particle identification. We select  $\Lambda_b$  decays by requiring a charged lepton and a  $\Lambda$  baryon with respective momentum  $> 3 \text{ GeV}$  and  $> 4 \text{ GeV}$  that are within  $\Delta R = \sqrt{(\Delta\eta)^2 + (\Delta\phi)^2} < 0.4$  of each other. The  $\Lambda$  baryon must have a decay radius  $> 3 \text{ cm}$ . The momentum requirements are the same as those used in the ALEPH b-baryon lifetime measurement [29], while the decay radius requirement is looser in order to maintain high acceptance. The corresponding increase in background would have to be mitigated by improved detector resolution or analysis algorithms. The acceptance of the momentum requirements is 81% per  $\Lambda_b$  baryon, and that of the decay radius is 45% per  $\Lambda_b$ . Incorporating these acceptances, a total of 210 reconstructed events is expected for a high-luminosity  $e^+e^-$  collider that produces 160 million Higgs boson events.

Sensitivity to the CP structure of the  $hbb$  vertex is obtained from the signed angle between the charged leptons in the Higgs boson rest frame:

$$\sin \delta\phi = \frac{\vec{p}_{\bar{\ell}} \cdot (\vec{p}_{\ell} \times \hat{p}_{\Lambda_b})}{\sqrt{(\vec{p}_{\ell})^2 - (\vec{p}_{\ell} \cdot \hat{p}_{\Lambda_b})^2} \sqrt{(\vec{p}_{\bar{\ell}})^2 - (\vec{p}_{\bar{\ell}} \cdot \hat{p}_{\Lambda_b})^2}}. \quad (3.1)$$

where  $\hat{p}_{\Lambda_b}$  represents the unit vector in the direction of  $\Lambda_b$ . The angle is reconstructed by taking the dijet momentum as a measure of the Higgs boson momentum, and the direction of each  $\Lambda_b$  baryon as the direction of the corresponding jet boosted into the Higgs boson rest frame. The difference between the baryon axis and the jet axis leads to a sign flip in  $\delta\phi$  in 31% of the events in the Monte Carlo. The asymmetry in these events will be cancelled by the same fraction of events without a sign flip, leaving 38% of the events available for a measurable asymmetry. Accounting for this reduction an asymmetry of 0.5 would be measurable at the  $3\sigma$  level. However, this is an order of magnitude larger than the maximum expected value of 0.04 given by eq. (2.44).

Given our optimistic assumptions in the collider luminosity and detector efficiencies and resolution, any CP test of the  $Hbb$  interaction using  $e^+e^-$  collisions appears unlikely. With a tenfold increase in yield from a 100 TeV  $\mu^+\mu^-$  collider, a test of the order of the maximum expected effect could be performed. Assuming the reconstruction acceptances are similar to those of an  $e^+e^-$  collider,  $2\sigma$  sensitivity could be possible for an asymmetry of 0.04.

### 3.2 $h \rightarrow c\bar{c} \rightarrow \Lambda_c\bar{\Lambda}_c$

The  $h \rightarrow c\bar{c}$  decay appears less promising than  $h \rightarrow b\bar{b}$  due to its 2.9% branching fraction. This is somewhat compensated by the fully reconstructible  $\Lambda_c \rightarrow pK\pi$  decay. The rate for  $c \rightarrow \Lambda_c \rightarrow pK\pi$  has been measured by ALEPH to be 0.39% [20], so only 0.44  $h \rightarrow \Lambda_c\bar{\Lambda}_c \rightarrow pK\pi pK\pi$  events are expected per million Higgs bosons produced. Even if we optimistically assume a reconstruction acceptance of 25% for each  $\Lambda_c$ , only 4.4 events would be expected at a high-luminosity  $e^+e^-$  collider. A high-luminosity  $\mu^+\mu^-$  collider could yield 40 events, which would provide  $1.5\sigma$  sensitivity to an asymmetry of 0.25. This is more than an order of magnitude larger than the maximum theoretical asymmetry of 0.02 using the  $\Lambda_c \rightarrow pK\pi$  decay.

## 4 Conclusion

In this work we have explored the feasibility of direct CP tests in Higgs-boson decays to heavy quarks in future collider experiments. The effect of a CP transformation is encoded at the fundamental level in relative complex phases for different helicity amplitudes, which we have converted into observables in angular distributions of the final decay particles. We have found that massive helicity amplitude methods are particularly well suited for tracing the spin correlations throughout the derivation of results.

A test of CP violation in these decays is challenging due to: *i*) the loss of measureable spin correlations during hadronization in all but the  $\Lambda_q$  channel, which has a  $< 10\%$  fragmentation

fraction; and *ii*) the low  $\Lambda_q$  branching ratio to experimentally reconstructible final states. The Higgs boson yields therefore need to be very high to approach sensitivity,  $\mathcal{O}(10^9)$  events, beyond the reach of all proposed colliders except a high-luminosity 100 TeV muon collider. With such a collider it may be possible to test maximal CP violation at the  $2\sigma$  level.

Due to the challenges in studying direct CP violation in  $h \rightarrow b\bar{b}$  decays, it is appropriate to study alternative tests such as the associated production of Higgs bosons with  $b$  or  $c$  quarks at hadron colliders, or the decay of the Higgs boson to  $J/\psi\gamma$ . By combining multiple approaches it may be possible to directly constrain CP violation in the  $hbb$  and  $hcc$  couplings.

## A Massive spinor conventions

The metric is taken in each  $SU(2)$  space as

$$(-\epsilon^{IJ}) = \epsilon^{\alpha\beta} = \epsilon^{\dot{\alpha}\dot{\beta}} = \begin{pmatrix} 0 & 1 \\ -1 & 0 \end{pmatrix}, \quad (\text{A.1})$$

and the helicity spinors are

$${}_{\alpha} |p^I\rangle = \left( \sqrt{E_p + |\vec{p}|} \begin{pmatrix} -s_{\theta/2} e^{-i\phi/2} \\ c_{\theta/2} e^{i\phi/2} \end{pmatrix}, \sqrt{E_p - |\vec{p}|} \begin{pmatrix} c_{\theta/2} e^{-i\phi/2} \\ s_{\theta/2} e^{i\phi/2} \end{pmatrix} \right) \quad (\text{A.2})$$

$${}^{\dot{\alpha}} |p^I] = \left( \sqrt{E_p - |\vec{p}|} \begin{pmatrix} -s_{\theta/2} e^{-i\phi/2} \\ c_{\theta/2} e^{i\phi/2} \end{pmatrix}, \sqrt{E_p + |\vec{p}|} \begin{pmatrix} c_{\theta/2} e^{-i\phi/2} \\ s_{\theta/2} e^{i\phi/2} \end{pmatrix} \right). \quad (\text{A.3})$$

The following relations are inferred from the above definitions

$$|p^I\rangle [p_I| = \sigma \cdot p \quad |p_I]\langle p^I| = \bar{\sigma} \cdot p \quad (\text{A.4})$$

$$[p^I p^J] = m\epsilon^{IJ} \quad \langle p^I p^J \rangle = -m\epsilon^{IJ} \quad (\text{A.5})$$

$$(\alpha |p^I\rangle)^* = {}_{\dot{\alpha}} |p_I] \quad ({}^{\dot{\alpha}} |p^I])^* = -{}^{\alpha} |p_I\rangle \quad (\text{A.6})$$

Finally we use the following prescription to turn an incoming particle into an outgoing one:

$$|-p^I\rangle = |p^I] \quad |-p^I] = -|p^I\rangle, \quad (\text{A.7})$$

so that  $|-p\rangle [-p| = -p \cdot \sigma$ .

## B Loss of spin correlation

As pointed out in Sec. 2.4, the CP-violation effect encoded in spin correlations vanishes if the combined fragmentation and decay yields a diagonal structure in spin indices. The simplest example of the loss of spin information is hadronization to a pseudoscalar meson. In this case eq. (2.8) leads to

$$\begin{aligned} \left( \mathcal{A}_{q \rightarrow P_q \rightarrow X} \mathcal{A}_{q \rightarrow P_q \rightarrow X}^{\dagger} \right)_J^I &= C \left( \langle q^I S_{\ell}^K \rangle + [S_{\ell}^K q^I] \right) \left( [S_{\ell, K} q_J] + \langle q_J S_{\ell, K} \rangle \right) \\ &= 2([q_J q^I] + \langle q^I q_J \rangle) = 4C m_q \delta_J^I \end{aligned} \quad (\text{B.1})$$



given that the spinor  $S_\ell$  is built with the momentum of  $q$ .

For the case of a vector meson decaying to a meson and a photon, as in the  $B^*$  case, one has

$$\begin{aligned} \left( \mathcal{A}_{q \rightarrow P_q^* \rightarrow P_q \gamma^+} \mathcal{A}_{q \rightarrow P_q^* \rightarrow P_q \gamma^+}^\dagger \right)_J^I &= C[S_\ell^L \gamma][q^I \gamma] \langle \gamma S_{\ell,L} \rangle \langle \gamma q_J \rangle = C \langle \gamma q_J \rangle [q^I \gamma] \left( -2p_\gamma \cdot p_{P_q^*} \right), \\ \left( \mathcal{A}_{q \rightarrow P_q^* \rightarrow P_q \gamma^-} \mathcal{A}_{q \rightarrow P_q^* \rightarrow P_q \gamma^-}^\dagger \right)_J^I &= C \langle S_\ell^L \gamma \rangle \langle q^I \gamma \rangle [\gamma S_{\ell,L}] [\gamma q_J] = C \langle \gamma q^I \rangle [q_J \gamma] \left( 2p_\gamma \cdot p_{P_q^*} \right). \end{aligned} \quad (\text{B.2})$$

Each term preserves q-quark polarization, but if the experiment is insensitive to photon helicity the sum gives

$$\begin{aligned} \langle q^I p_\gamma q_J \rangle - \langle q_J p_\gamma q^I \rangle &= \text{Tr} \left( p_\gamma \varepsilon_{JJ'} \left( |q^K \rangle \langle q^I| - |q^I \rangle \langle q^K| \right) \right) = \text{Tr} \left( p_\gamma |q_K \rangle \langle q^K| \right) \delta_J^I \\ &= 2p_\gamma \cdot p_q \delta_J^I \end{aligned} \quad (\text{B.3})$$

The decay to a polarized photon has a spin resolution power of 1 and the fragmentation into  $P_q^*$  is  $\approx 7$  [37] greater than to  $\Lambda_q$  baryons. If such decays could be observed in a future experiment they would provide a promising avenue for a CP test of the  $hbb$  interaction.

The above two cases summarize the possible structures of a two-body decay of an excited hadron via the QCD or QED interaction. Using only parity one can write in general

$$\begin{aligned} \mathcal{A}_{q \rightarrow H} \left( \sum_{s_X, s_Y} d\Gamma_{H \rightarrow XY} \right) \mathcal{A}_{q \rightarrow H}^\dagger &= S(\langle q^I q_J \rangle - [q^I q_J]) + J^\mu (\langle q^I \sigma^\mu q_J \rangle - \langle q_J \sigma_\mu q^I \rangle) \\ &= (2m_q S + 2J \cdot p_q) \delta_J^I. \end{aligned} \quad (\text{B.4})$$

To build the parity-even structure one can start from two incoming  $q^I$  and  $\bar{q}^J$  quarks as in eq. (2.5) for Higgs-boson decay and flip the momentum of  $\bar{q}$  to turn it into an outgoing quark, which gives the relative sign in eq. (A.7).

## C Polarization resolution

The spin resolution power  $\alpha$  is determined using the following integrals:

$$I_\Lambda = \int \hat{f}_{1c}^2(x) \frac{(1 - \delta + x)^2 - 4x}{48} (2x + \delta - 1) dx \quad (\text{C.1})$$

$$I_{\ell, in} = \int \frac{y-x}{16} \left( 1 - \delta - \frac{2x}{y} + x - y \right) \Theta(z) dx dy \quad (\text{C.2})$$

$$I_{\ell, ex} = \int \hat{f}_{1q}^2(x) \frac{y-x}{16} \left( 1 - \delta - \frac{2x}{y} + x - y \right) \Theta(z) dx dy \quad (\text{C.3})$$

with  $z = 1 + x - \delta - x/y - y$ ,  $\Theta$  the heaviside function, and the limits of integration in the first integral given by  $x = 0, (1 - \sqrt{\delta})^2$ . To obtain the resolution power these integrals are divided by the appropriate integral,

$$I_{in} = \int \frac{1}{16} (y-x)(1+x-\delta-y) \Theta(z) dx dy \quad (\text{C.4})$$

$$I_{ex} = \int \hat{f}_{1q}^2(x) \frac{1}{16} (y-x)(1+x-\delta-y) \Theta(z) dx dy. \quad (\text{C.5})$$

In these integrals we model the semi-leptonic decay form factor using the Isgur-Wise function [38],

$$f(x) = \frac{\omega_0^2}{\omega_0^2 + \frac{(1-\sqrt{\delta})^2-x}{\sqrt{\delta}}} \quad (\text{C.6})$$

with  $\omega_0 = 0.89$ . The spin resolution powers are given by

$$\alpha = \frac{I_{\ell,in}}{I_{in}} \quad \alpha = \frac{I_{\ell,ex}}{I_{ex}} \quad \alpha = \frac{I_{\Lambda}}{I_{ex}}. \quad (\text{C.7})$$

## References

- [1] ATLAS Collaboration, *Higgs boson production cross-section measurements and their EFT interpretation in the  $4\ell$  decay channel at  $\sqrt{s} = 13$  TeV with the ATLAS detector*, *Eur. Phys. Jour. C* **80** (2020) 957.
- [2] CMS Collaboration, *Measurements of the Higgs boson width and anomalous HVV couplings from on-shell and off-shell production in the four-lepton final state*, *Phys. Rev. D* **99** (2019) 112003.
- [3] CMS Collaboration, *Analysis of the CP structure of the Yukawa coupling between the Higgs boson and  $\tau$  leptons in proton-proton collisions at  $\sqrt{s} = 13$  TeV*, *CMS-PAS-HIG-20-006* (2020).
- [4] ATLAS Collaboration, *CP Properties of Higgs Boson Interactions with Top Quarks in the  $t\bar{t}H$  and  $tH$  Processes Using  $H \rightarrow \gamma\gamma$  with the ATLAS Detector*, *Phys. Rev. Lett.* **125** (2020) 061802.
- [5] CMS Collaboration, *Measurements of  $t\bar{t}H$  Production and the CP Structure of the Yukawa Interaction between the Higgs Boson and Top Quark in the Diphoton Decay Channel*, *Phys. Rev. Lett.* **125** (2020) 061801, [[arXiv:2003.10866](https://arxiv.org/abs/2003.10866)].
- [6] A. V. Manohar and M. B. Wise, *Heavy quark physics*, vol. 10. Cambridge University Press, 2000.
- [7] A. F. Falk and M. E. Peskin, *Production, decay, and polarization of excited heavy hadrons*, *Phys. Rev. D* **49** (1994) 3320, [[hep-ph/9308241](https://arxiv.org/abs/hep-ph/9308241)].
- [8] Y. Grossman and D. Pirjol, *Extracting and using photon polarization information in radiative B decays*, *Journal of High Energy Physics* **06** (2000) 029.
- [9] ALEPH Collaboration, *Measurement of the  $\Lambda_b$  polarization in Z decays*, *Phys. Lett. B* **365** (1996) 437.
- [10] OPAL Collaboration, *Measurement of the average polarization of b baryons in hadronic  $Z^0$  decays*, *Phys. Lett. B* **444** (1998) 539.
- [11] DELPHI Collaboration,  *$\Lambda_b$  polarization in  $Z^0$  decays at LEP*, *Phys. Lett. B* **474** (2000) 205.
- [12] M. Galanti, A. Giammanco, Y. Grossman, Y. Kats, E. Stamou, and J. Zupan, *Heavy baryons as polarimeters at colliders*, *Jour. High En. Phys.* **11** (2015) 67.
- [13] R. Kleiss and W. J. Stirling, *Spinor Techniques for Calculating  $p\bar{p} \rightarrow W^\pm/Z^0 + \text{Jets}$* , *Nucl. Phys. B* **262** (1985) 235–262.

- [14] R. Kleiss and W. J. Stirling, *Top quark production at hadron colliders: Some useful formulae*, *Z. Phys. C* **40** (1988) 419.
- [15] N. Arkani-Hamed, T.-C. Huang, and Y. Huang, *Scattering Amplitudes For All Masses and Spins*, [arXiv:1709.04891](#).
- [16] DELPHI Collaboration, *A study of the b-quark fragmentation function with the DELPHI detector at LEP I and an averaged distribution obtained at the Z Pole*, *Eur. Phys. J. C* **71** (2011) 1557.
- [17] J. D. Bjorken, *Spin Dependent Decays of the Lambda(c)*, *Phys. Rev. D* **40** (1989) 1513.
- [18] M. Jezabek, K. Rybicki, and R. Rylko, *Experimental study of spin effects in hadroproduction and decay of Lambda(c)+*, *Phys. Lett. B* **286** (1992) 175–179.
- [19] **Heavy Flavor Averaging Group (HFAG)** Collaboration, Y. Amhis et al., *Averages of b-hadron, c-hadron, and  $\tau$ -lepton properties as of summer 2014*, [arXiv:1412.7515](#).
- [20] ALEPH Collaboration, *Study of charm production in Z decays*, *Eur. Phys. Jour. C* **16** (2000) 597.
- [21] A. Abada *et al.* (FCC Collaboration), *FCC-hh: The Hadron Collider*, *Eur. Phys. Jour. Sp. Top.* **228** (2019) 755.
- [22] R. Contino *et al.*, *Physics at a 100 TeV pp collider: Higgs and EW symmetry breaking studies*, [arXiv:1606.09408](#).
- [23] P.A. Zyle *et al.* (Particle Data Group), *Review of Particle Physics*, *Prog. Theor. Exp. Phys.* **2020** (2020) 083C01.
- [24] A. Abada *et al.* (FCC Collaboration), *FCC-ee: The Lepton Collider*, *Eur. Phys. Jour. Sp. Top.* **228** (2019) 261.
- [25] V. N. Litvinenko, T. Roser, and M. Chamizo-Llatas, *High-energy high-luminosity  $e^+e^-$  collider using energy-recovery linacs*, *Phys. Lett. B* **804** (2020) 135394.
- [26] J. P. Delahaye *et al.*, *Muon Colliders*, [arXiv:1901.06150](#).
- [27] H. A. Ali *et al.*, *The Muon Smasher’s Guide*, [arXiv:2103.14043](#).
- [28] A. Costantini, F. De Lillo, F. Maltoni, L. Mantani, O. Mattelaer, R. Ruiz, and X. Zhao, *Heavy baryons as polarimeters at colliders*, *Jour. High En. Phys.* **9** (2020) 80.
- [29] ALEPH Collaboration, *Measurement of the b baryon fraction and lifetime in Z decays*, *Eur. Phys. Jour. C* **2** (1998) 197.
- [30] DELPHI Collaboration, *Measurement of the lifetime of b-baryons*, *Eur. Phys. Jour. C* **10** (1999) 185.
- [31] OPAL Collaboration, *Measurement of the average b-baryon lifetime and the product branching ratio  $f(b \rightarrow \Lambda_b) \cdot BR(\Lambda_b \rightarrow \Lambda \ell^- \bar{\nu} X)$* , *Z. Phys. C* **69** (1996) 195.
- [32] ATLAS Collaboration, *Observation of  $H \rightarrow b\bar{b}$  decays and  $VH$  production with the ATLAS detector*, *Phys. Lett. B* **786** (2018) 59.
- [33] CMS Collaboration, *Observation of Higgs Boson Decay to Bottom Quarks*, *Phys. Rev. Lett.* **121** (Sep, 2018) 121801.
- [34] P. Azzi *et al.*, *Prospective Studies for LEP3 with the CMS Detector*, [arXiv:1208.1662](#).

- [35] J. Allwall *et al.*, *The automated computation of tree-level and next-to-leading order differential cross sections, and their matching to parton shower simulations*, *Jour. High En. Phys.* **7** (2014) 79.
- [36] T. Sjöstrand, S. Mrenna, and P. Skands, *PYTHIA 6.4 physics and manual*, *Jour. High En. Phys.* **05** (2006) 026.
- [37] M. Feindt, *B quark fragmentation*, in *30th Rencontres de Moriond: QCD and High-energy Hadronic Interactions*, 1995.
- [38] T. Mannel, W. Roberts, and Z. Ryzak, *A Derivation of the heavy quark effective Lagrangian from QCD*, *Nucl. Phys. B* **368** (1992) 204.